THE JOURNAL OF BIOLOGICAL CHEMISTRY VOL. 289, NO. 33, pp. 23004–23019, August 15, 2014

The Serotonin Transporter Undergoes Constitutive Internalization and Is Primarily Sorted to Late Endosomes and Lysosomal Degradation*

Received for publication, December 20, 2013, and in revised form, June 16, 2014 Published, JBC Papers in Press, June 27, 2014, DOI 10.1074/jbc.M113.495754

Troels Rahbek-Clemmensen[‡§1], **Tina Bay**[‡1], **Jacob Eriksen**[‡§], **Ulrik Gether**[‡§2], **and Trine Nygaard Jørgensen**[‡]

From the [‡]*Molecular Neuropharmacology Laboratory, Department of Neuroscience and Pharmacology, Faculty of Health Sciences, Panum Institute, and the* [§]*Lundbeck Foundation Center for Biomembranes in Nanomedicine, University of Copenhagen, DK-2200 Copenhagen, Denmark*

Background: SERT is a target for antidepressants, but little is known about its constitutive cellular trafficking properties.
Results: SERT undergoes marked constitutive internalization, and internalized SERT co-localizes primarily with markers of the late endosomal/lysosomal pathway.
Conclusion: SERT is primarily sorted to degradation rather than to recycling.
Significance: The findings are important for our general understanding of how SERT regulates serotonin signaling.

The serotonin transporter (SERT) plays a critical role in regulating serotonin signaling by mediating reuptake of serotonin from the extracellular space. The molecular and cellular mechanisms controlling SERT levels in the membrane remain poorly understood. To study trafficking of the surface resident SERT, two functional epitope-tagged variants were generated. Fusion of a FLAG-tagged one-transmembrane segment protein Tac to the SERT N terminus generated a transporter with an extracellular epitope suited for trafficking studies (TacSERT). Likewise, a construct with an extracellular antibody epitope was generated by introducing an HA (hemagglutinin) tag in the extracellular loop 2 of SERT (HA-SERT). By using TacSERT and HA-SERT in antibody-based internalization assays, we show that SERT undergoes constitutive internalization in a dynamin-dependent manner. Confocal images of constitutively internalized SERT demonstrated that SERT primarily co-localized with the late endosomal/lysosomal marker Rab7, whereas little co-localization was observed with the Rab11, a marker of the "long loop" recycling pathway. This sorting pattern was distinct from that of a prototypical recycling membrane protein, the β_2-adrenergic receptor. Furthermore, internalized SERT co-localized with the lysosomal marker LysoTracker and not with transferrin. The sorting pattern was further confirmed by visualizing internalization of SERT using the fluorescent cocaine analog JHC1-64 and by reversible and pulse-chase biotinylation assays showing evidence for lysosomal degradation of the internalized transporter. Finally, we found that SERT internalized in response to stimulation with 12-myristate 13-acetate co-localized primarily with Rab7- and LysoTracker-positive compartments. We conclude that SERT is constitutively internalized and that the internalized transporter is sorted mainly to degradation.

The serotonin transporter (SERT)[3] is responsible for reuptake of the neurotransmitter serotonin (5-HT) following its release from the presynaptic nerve terminal. SERT plays a major role in regulating serotonergic signaling, and alterations in its function have been linked to several psychiatric disorders such as depression, anxiety, obsessive-compulsive disorder, autism, and alcohol abuse. Furthermore, SERT has been the subject of intensive research efforts as the target for antidepressant drugs such as citalopram (Cipralex/Lexapro) and fluoxetine (Prozac) as well as for psychostimulant drugs such as cocaine and 3,4-methylenedioxymethamphetamine ("Ecstasy") (1–3). SERT belongs to the solute carrier (SLC) 6 gene family that also includes transporters for the neurotransmitters dopamine, norepinephrine, glycine, and γ-aminobutyric acid (GABA) (1–3). Members of this family share a predicted structure with 12 transmembrane domains and intracellular N and C termini. This topology was first confirmed by the high resolution crystal structure of the bacterial homolog, LeuT, of the mammalian SLC6 transporters (4) and recently by a high resolution structure of the *Drosophila* dopamine transporter (5).

Because of the central role of SERT in maintaining brain 5-HT homeostasis, it is critical to understand the molecular and cellular mechanisms that control the level of SERT protein in the plasma membrane. A well described regulatory mechanism is the effect of phorbol esters, such as phorbol 12-myristate 13-acetate (PMA) on SERT membrane availability. Upon stimulation with PMA, leading to activation of protein kinase C (PKC) as well as other kinases, SERT undergoes marked inter-

* This work was supported, in whole or in part, by National Institutes of Health Grant P01 DA 12408. This work was also supported by the Danish Medical Research Council, University of Copenhagen BioScaRT Program of Excellence, Lundbeck Foundation Center for Biomembranes in Nanomedicine, Novo Nordisk Foundation, and Fabrikant Vilhelm Pedersen og Hustrus Mindelegat.

[1] Both authors contributed equally to this work.

[2] To whom correspondence should be addressed: Dept. of Neuroscience and Pharmacology, Panum Institute 18.6, Blegdamsvej 3, DK-2200 Copenhagen N, Denmark. Tel.: 45-23840089; Fax: 45-35327610; E-mail: gether@sund.ku.dk.

[3] The abbreviations used are: SERT, serotonin transporter; 5-HT, 5-hydroxytryptamine; PMA, phorbol 12-myristate 13-acetate; ANOVA, analysis of variance; hSERT, human SERT; EGFP, enhanced GFP; β_2-AR, β_2-adrenergic receptor; DAT, dopamine transporter; GLYT2, glycine transporter 2; SLC, solute carrier; GABA, gamma-aminobutyric acid; CAD cells, Cath.a-differentiated cells; Tf-488, Alexa-Fluor 488-conjugated transferrin.

nalization (6, 7). The effect of phorbol ester stimulation on transporter surface expression seems to be a common regulatory mechanism for the SLC6 family (3). In addition, a range of additional kinases, various interacting proteins, as well as substrates and inhibitors has been found to regulate SLC6 neurotransmitter transporter internalization (1, 3, 8, 9). Interestingly, some SLC6 family members, *e.g.* the dopamine transporter (DAT) and the glycine transporter 2 (GLYT2), were found also to undergo a marked constitutive internalization (10–12).

A major and yet not fully resolved question is the fate of the SLC6 transporters following both regulated and constitutive internalization. Indeed, internalization serves an important role in sorting different membrane proteins to different cellular destinations. Some membrane proteins such as the transferrin receptor and the G-protein-coupled β_2-adrenergic receptor are efficiently recycled back to the plasma membrane upon constitutive and agonist-induced internalization, respectively (13, 14). Other membrane proteins such as the EGF receptor and the δ-opioid receptor are destined to late endosomes and lysosomes for degradation upon endocytosis (14, 15). For the SLC6 transporters, it has been suggested based on use of recycling inhibitors that both DAT and the glycine transporter 2 (GLYT2) are sorted to a recycling pathway, permitting reinsertion in the membrane (11, 12, 16). It was therefore proposed that internalization of these transporters serve to maintain an intracellular pool of transporters that can be recruited to the surface during periods of high signaling activity (12). Recently, we characterized in detail postendocytic sorting of DAT by use of co-expressed markers of distinct endocytic compartments and found that constitutively internalized DAT is sorted to a late endosomal/lysosomal degradative pathway as well as in part to a "short loop" Rab4-positive recycling pathway in both neurons and cell lines. Of interest, we observed little evidence for recycling of DAT via the "long loop" Rab11-positive recycling compartment that is utilized by *bona fide* recycling receptors, such as the β_2-adrenergic receptor (17).

In contrast to the rather detailed information available about DAT, little is known about the trafficking properties and postendocytic sorting pattern of SERT. Given the poor sequence identity between DAT and SERT in the intracellular N and C termini, it is conceivable that the two proteins might be subject to differential cellular regulation and thus that they are not following the same intracellular trafficking pathways. To study the trafficking properties of SERT, we used five different approaches as follows: 1) a fusion protein of SERT and the FLAG-tagged single transmembrane segment protein Tac (TacSERT), providing an extracellular antibody epitope for dynamic visualization of internalization; 2) a SERT construct with an HA tag inserted into the second extracellular loop, thereby also providing an extracellular antibody epitope (HA-SERT); 3) a fluorescent cocaine analog (JHC1-64) allowing visualization of SERT in live cells (18); 4) a reversible biotinylation assay permitting biochemical assessment of SERT trafficking; and 5) a "pulse-chase" biotinylation experiment enabling assessment of SERT degradation over time. By exploiting these approaches, we establish that SERT, like DAT, undergoes marked constitutive internalization. Moreover, we visualized and quantified co-localization between internalized SERT and a series of intracellular markers. The experiments showed that SERT is postendocytically sorted preferentially to Rab7-positive late endosomes and only to a limited degree to the Rab11-mediated recycling pathway. Sorting to a degradative pathway was further supported by reversible biotinylation and pulse-chase biotinylation, showing that blocking of lysosomal degradation led to increased accumulation of internalized SERT. Finally, we demonstrate that SERT internalized in response to PMA stimulation also seems to favor the same postendocytic pathway as constitutively internalized SERT. These observations shed new light on the trafficking properties of SERT and should prove important for our general understanding of how SERT regulates serotonin signaling under both physiological and pathophysiological conditions.

EXPERIMENTAL PROCEDURES

Molecular Biology—The coding sequence of hSERT was inserted into the mammalian expression vector pcDNA3.1(−) (Invitrogen) using XbaI and HindIII restriction sites. To generate HA-tagged SERT, residues 212–215 (YFSE) in the EL2 of hSERT were replaced by the sequence YPYDVPDUASL (HA epitope is underlined) by a two-step PCR. The PCR product was ligated into the pcDNA3.1 hSERT construct using BlpI and AgeI digestion. The construct was verified by automatic dideoxynucleotide sequencing. TacSERT was generated as described in Ref. 19 and c-Myc-SERT as described in Ref. 20. Tac and TacDAT in pcDNA3 were described in Ref. 17. The EGFP-tagged Rab7 and Rab11 constructs (pEGFP-C1 Rab7 and pEGFP-C1 Rab11) were kindly provided by Dr. Kathrine W. Roche, NINDS, National Institutes of Health, Bethesda, MD (21). The pEGFP-Rab4 plasmid was a kind gift from Dr. José A. Esteban, Universidad Autónoma de Madrid, Madrid, Spain (22). The FLAG-β_2-adrenergic receptor in pcDNA3.1 was a kind gift from Dr. Mark von Zastrow, University of California at San Francisco. The cDNAs encoding dynamin and the dominant negative dynamin mutant K44A were kind gifts from Sandra Schmid, The Scripps Research Institute, La Jolla, CA.

Cell Cultures and Transfections—Human embryonic kidney (HEK293) cells (ATCC CRL-1573) were grown in Dulbecco's modified Eagle's medium (DMEM) with HEPES and sodium bicarbonate and Cath.a-differentiated (CAD) cells (23) in Ham's F-12/DMEM (1:1) (Invitrogen), both supplemented with 10% (v/v) fetal bovine serum (FBS) (Invitrogen) and 0.01 mg/ml gentamicin (Invitrogen), in the presence of 5% CO_2 in a 95% humidified atmosphere at 37 °C. 24 h prior to transfection, 4×10^6 HEK293 or CAD cells were plated in a 75-cm^2 culture flask in medium without gentamicin. Transient transfection was performed using LipofectAMINE2000 (Invitrogen) according to the manufacturer's instructions. The DNA/LipofectAMINE2000 ratio used was 1:3, using 1–2 $\mu g/\mu l$ DNA.

Primary Antibodies—Mouse anti-HA.11 and mouse M1 anti-FLAG were from Covance (Princeton, NJ) and Sigma, respectively. Primary AlexaFluor-conjugated M1 and HA.11 antibodies were generated using the APEX™ Alexa Fluor® 568 antibody labeling kit according to the manufacturer's manual (Invitrogen). M1 and HA.11 fluorophore-conjugated antibodies were used 1:1000 and 1:200, respectively. Mouse anti-c-Myc

and HRP-conjugated anti-β-actin were from Sigma. Secondary AlexaFluor-conjugated antibodies for immunocytochemistry were from Molecular Probes (Eugene, OR). Secondary HRP-conjugated goat anti-mouse antibody was from Pierce, and secondary antibody HRP-conjugated goat anti-mouse was from Chemicon (Billerica, MA).

Antibody Feeding Internalization Assay—CAD cells or HEK293 cells transiently expressing Tac, TacSERT, or HA-SERT (and EGFP-dynamin I/K44A) were plated on polyornithine-coated coverslips in 6-well plates with a density of 400,000 cells/well. 2 days after transfection, cells were incubated for 1 h with Alexa568 M1-conjugated antibody (1:1000) at 4 °C to label FLAG constructs or Alexa568 HA.11-conjugated antibody (and 1:200) at 18 °C to label HA-SERT in the cell line's respective media. Afterward, the cells were incubated in fresh medium for 30–60 min at 37 °C allowing internalization (or at 4 °C for a nontrafficking surface control), followed by two washes in ice-cold phosphate-buffered saline (PBS). Cells were then fixed in 4% paraformaldehyde for 15 min at 0 °C. Finally, the cells were mounted in ProLong Gold Antifade reagent (Molecular Probes, Invitrogen) and visualized by confocal microscopy. When assessing the influence of PMA on internalization, at the time of internalization the cells were incubated with 1 μM PMA at 37 °C (or 4 °C for surface control).

JHC1-64 Internalization Assay—For visualizing internalization using the fluorescent cocaine analog JHC1-64, the CAD or HEK293 cells transiently expressing hSERT were used 48 h after transfection. The cells were incubated with 20 nM JHC1-64 in serum-free medium for 30 min at 15 °C, allowing JHC1-64 to bind to SERT while blocking internalization. The cells were washed in medium to remove excess JHC1-64 before internalization was allowed by incubating for 1 h at 37 °C. Specific binding of JHC1-64 to hSERT was validated by incubating CAD cells transiently expressing EGFP-SERT with 10 nM JHC1-64 for 10 min followed by washing twice in serum-free medium and imaging by confocal microscopy. To block binding of JHC1-64 to hSERT, cells were incubated with 1 μM of the SERT-specific inhibitor paroxetine for 10 min before addition of 10 nM JHC1-64.

Co-localization Assay of SERT with Endosomal Markers—For co-localization experiments, CAD cells were transfected with equal amounts of TacSERT, HA-SERT, or FLAG-β_2-AR and either EGFP-Rab4, EGFP-Rab-7, or EGFP-Rab11 (1:1). At least 24 h post-transfection, the antibody feeding or JHC1-64 internalization assay was performed as described above. For assaying co-localization of the β_2-AR, 10 μM isoproterenol was added during the time of internalization to induce receptor endocytosis. To visualize early and recycling endosomes during the time of internalization, cells were incubated with Alexa-Fluor 488-conjugated transferrin (Tf-488) (1:100; Invitrogen) 10 min prior to fixation. Likewise, to visualize lysosomes, cells were incubated with LysoTracker Green (50 nM, Invitrogen) prior to fixation.

Confocal Microscopy—Confocal microscopy was performed using a Zeiss LSM 510 laser-scanning unit (Carl Zeiss, Oberkochen, Germany) and an inverted microscope with an oil immersion 63 × 1.4 numerical aperture objective (Carl Zeiss). Alexa488 and EGFP were excited using a 488-nm laser line from an argon-krypton laser, and detection of the emitted light was filtered using a long pass 505–530-nm barrier filter. The Alexa568 dye as well as rhodamine-labeled JHC1-64 were excited using a 543-nm helium-neon laser, and fluorescence was cleaned up using a 560-nm long pass filter. Images were collected in 512 × 512 or 1024 × 1024 pixels, and pinholes were set to achieve optical sections of 1 μm. Signal collection was set to avoid saturation, and images were combined using ImageJ software.

Co-localization Quantification—Co-localization of EGFP-tagged Rab4, Rab7, and Rab11 with TacSERT, HA-SERT, and β_2-adrenerigc receptor was quantified using the RG2B co-localization plug-in to ImageJ as described previously (24). The region of interest was confined to single cells to avoid background noise. A minimum threshold pixel intensity of 100 was set for each channel, and the minimum ratio for pixel intensity between the two channels was set to 0.5. Co-localization is displayed as percentage of co-localizing pixel by the total area divided by the threshold of the M1 or HA.11 signal. Approximately 25–35 cells were used for quantification under each condition. Statistical significance was determined by one-way ANOVA followed by Bonferroni's multiple comparison test.

ELISA-based Internalization Assay—CAD cells were transiently transfected with Tac, TacSERT, or TacDAT. When assessing dynamin dependence, TacSERT was co-transfected with dynamin I, the dominant negative dynamin I (K44A), or pcDNA3.1. Cells were first incubated for 1 h at 4 °C in cold serum-free DMEM with primary M1 antibody (1:5000) added to each well. Subsequently, cells were washed four times in DMEM/F-12 (1:1, referred to as media), and then warm (37 °C) media were added, and cells were incubated at 37 °C for 1 h allowing internalization or at 4 °C for 1 h in the control situation. When indicated, 1 μM PMA was added to the media during this step. To remove surface-bound M1, cells were incubated with an acidic strip buffer (0.5 M NaCl, 0.2 M acetic acid) for 10 min on ice (PBS used as control), then washed twice with PBS, fixed in 4% paraformaldehyde in PBS for 10 min, and again washed twice in PBS. Then the cells were blocked for 30 min in blocking buffer (PBS + 5% goat serum) and permeabilized in blocking buffer with 0.1% saponin for 30 min. Cells were then incubated with secondary HRP-conjugated goat anti-mouse antibody (1:1000) in blocking buffer for 30 min and washed four times in PBS. Cells were incubated with SuperSignal ELISA Femto maximum sensitivity substrate (Pierce) for 30 s with shaking before luminescence was detected on a Wallac Victor2.

Surface ELISA—CAD cells transiently transfected with Tac, TacSERT, or β_2-AR were incubated with 25 μM monensin for 1 h at 37 °C prior to the assay. 10 μM isoproterenol was added to β_2-AR-expressing cells to induce receptor internalization. Cells were washed in ice-cold PBS, fixated in 4% paraformaldehyde, washed twice in PBS, and blocked for 30 min with 5% goat serum in PBS (blocking buffer). Subsequently, cells were incubated for 30 min with primary antibody M1 (1:5000) in blocking buffer at room temperature. The cells were washed four times in PBS and then incubated for 30 min in HRP-conjugated goat anti-mouse antibody (IgG) (1:1000) in blocking buffer at room temperature, followed by four washes in PBS. Cells were incu-

bated with SuperSignal ELISA Femto Maximum Sensitivity Substrate (Pierce) as described above.

5-[^{3}H]HT Uptake—Saturation kinetics of 5-HT uptake was determined using an increasing concentration of 5-HT with a trace amount of 5-hydroxy[^{3}H]tryptamine trifluoroacetate (5-[^{3}H]HT) (GE Healthcare). 24 h prior to uptake assay, CAD cells transiently transfected with HA-SERT were plated in 24-well plates with a density of 200,000 cells per well. On the day of the experiment (48 h after transfection), cells were washed once in 1 ml of 37 °C uptake buffer (25 mM HEPES, 120 mM sodium chloride, 5 mM potassium chloride, 1.2 mM calcium chloride, and 1.2 mM magnesium sulfate supplemented with 10 mM D-glucose, 1 mM ascorbic acid, and 1 μM pargyline, pH 7.4) and equilibrated in 450 μl of uptake buffer per well for 20 min at 37 °C. Uptake was initiated by adding serial dilutions of 5-HT: 5-[^{3}H]HT with final concentrations of 6.4 to 0.05 μM. Uptake was allowed for 3 min at room temperature with shaking and was terminated by washing twice in ice-cold uptake buffer. Cells were first lysed in 1% SDS and subsequently transferred to cell counting plates (PerkinElmer Life Sciences) where Optiphase HiSafe 3scintillation fluid (PerkinElmer Life Sciences) was added. Radioactivity was measured in a Wallac Tri-Lux β scintillation counter (PerkinElmer Life Sciences). Nonspecific uptake (defined as background) was determined in the presence of 0.2 μM paroxetine, added during equilibration in uptake buffer for 20 min at 37 °C. Background corrected data were analyzed in GraphPad Prism 5.0 (GraphPad Software, San Diego). All determinations were performed in triplicate.

Reversible Biotinylation Assay—For reversible biotinylation, 500,000 CAD cells transiently expressing c-Myc-SERT were seeded in 6-well plates 24 h prior to the experiment. On the day of the experiment, the cells were incubated for 1 h with 0.6 mg/ml sulfo-NHS-S-S-biotin in PBS on ice. Prior to internalization, the cells were washed twice with ice-cold 100 mM glycine in PBS and twice with ice-cold PBS to remove unbound sulfo-NHS-S-S-biotin. Subsequently, two wells were kept on ice, while the four other wells were incubated for 2 h in warm media at 37 °C with no extra treatment, 10 μg/ml leupeptin, 10 μg/ml leupeptin + 200 μM chloroquine, or 10 μg/ml leupeptin + 25 μM monensin. Chloroquine was only present for 90 min. All samples were washed in ice-cold PBS. To remove surface biotin, all but the "total surface" sample was treated twice with 100 mM MesNA, 0.2% bovine serum albumin, 50 mM Tris-HCl, pH 8.8, 100 mM NaCl, 1 mM EDTA, for 20 min and subsequently washed twice in ice-cold PBS. Samples were lysed in lysis buffer (25 mM Tris, pH 7.5, 100 mM NaCl, 1 mM EDTA, 1% Triton X-100, 0.2 mM PMSF, protease inhibitor mixture (Roche Applied Science), and 5 mM *N*-ethylmaleimide), mixed for 20 min at 4 °C, and centrifuged for 15 min at 16,000 × *g* at 4 °C to remove cell debris. A total sample was collected from all samples and mixed with an equal volume of 2× loading buffer containing 1% SDS, 2.5% β-mercaptoethanol, and 100 mM dithiothreitol (DTT). For pulldown of biotinylated proteins, the samples were loaded on avidin beads, mixed overnight at 4 °C, then washed four times in lysis buffer with a 3-min centrifugation at 3000 × *g* per wash, and incubated for 30 min with 2× loading buffer. To remove the avidin beads, the sample was filtered before analysis by SDS-PAGE. Each sample was loaded and analyzed on a 10% pre-stacked gel (Bio-Rad), followed by blotting to a PDVF membrane (Millipore, MA) and developing with various primary antibodies as follows: mouse anti-c-Myc 1:1000, HRP-conjugated anti-β-actin 1:20,000 in 5% milk powder, 0.05% Tween 20 in PBS. Secondary antibody was HRP-conjugated goat anti-mouse 1:5000. Finally, the membrane was developed with ECL prime Western blotting reagent (GE Healthcare). Immunoreactivity was quantified using ImageJ. Statistical significance was determined by one-way ANOVA followed by Bonferroni's multiple comparisons test.

Pulse-Chase Biotinylation Assay—HEK293 cells (~900,000) were transiently transfected with c-Myc-SERT and seeded in 6-well plates 1 day prior to the experiment. On the day of the experiment, cells were incubated for 15 min on ice with 1.2 mg/ml sulfo-NHS-biotin in PBS followed by washing twice with 100 mM glycine in PBS to stop the reaction. One well was lysed in lysis buffer to determine the cell surface before internalization. Two other wells were washed once in prewarmed (37 °C) media (DMEM with HEPES), added to prewarmed media ± 100 μg/ml leupeptin, and incubated for 4 h at 37 °C. The cells were collected in lysis buffer (25 mM Tris, pH 7.5, 100 mM NaCl, 1 mM EDTA, 1% Triton X-100, 0.2 mM PMSF, protease inhibitor mixture (Roche Applied Science), and 5 mM *N*-ethylmaleimide), mixed for 20 min at 4 °C, and centrifuged for 15 min at 16,000 × *g* at 4 °C to remove cell debris. For isolation of biotinylated protein, the samples were loaded on streptavidin beads, mixed overnight at 4 °C, and then washed four times in lysis buffer with 3 min of centrifugation at 3000 × *g* per wash. To elute biotinylated protein from the streptavidin beads, each sample was incubated for 4 min at 60 °C with an equal volume of 2× loading buffer containing 2.5% SDS, 10% β-mercaptoethanol, and 300 mM DTT. Each sample was analyzed by Western blotting as described for reversible biotinylation. Immunoreactivity was quantified using ImageJ. Statistical significance was determined using a *t* test.

RESULTS

Serotonin Transporter Is Constitutively Internalized—It has proven notoriously difficult to generate a highly specific antibody specifically directed to any part of the extracellular sequence of SERT, and to our knowledge such an antibody is not available. Accordingly, it has not been possible to monitor SERT endocytosis directly and in live cells in antibody feeding experiments using fluorescently labeled antibodies, for example. To solve this problem, we used a construct in which the single transmembrane protein Tac was fused to the N terminus of SERT, resulting in a SERT variant with an extra transmembrane domain (19). The construct was modified to contain an extracellular FLAG epitope (DYKDDDDK) at the Tac N terminus preceded by a signal peptide (Fig. 1*A*). After cleavage of the signal peptide, the epitope can be detected by the highly specific anti-FLAG antibody M1. As we described previously, this construct, TacSERT, exhibits normal functional activity with 5-HT uptake and inhibitor binding properties that are not significantly different from those of the wild type hSERT (19). Furthermore, immunolabeling followed by confocal microscopy showed that TacSERT was homogeneously distributed at the

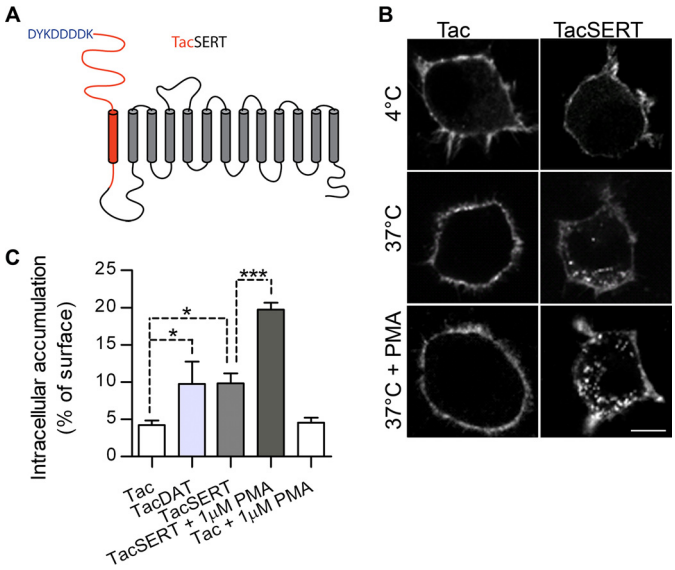

FIGURE 1. **TacSERT is constitutively internalized in CAD cells.** *A*, topology diagram of TacSERT, a chimeric protein of the interleukin 2 receptor α subunit (Tac) fused to the N terminus of SERT. An N-terminal FLAG epitope was added to the extracellular domain of Tac. *B*, antibody feeding internalization assay. Confocal images of CAD cells expressing FLAG-tagged Tac or TacSERT detected by Alexa568-conjugated M1. After incubation with the antibody at 4 °C, cells were either kept at 4 °C (no trafficking) or at 37 °C for 30 min to allow internalization. When indicated, 1 μM PMA was added during the 37 °C incubation. *Scale bar,* 10 μm. *C*, intracellular accumulation detected by ELISA-based internalization assay. Cells transiently transfected with Tac, TacDAT, or TacSERT were labeled with M1 at 4 °C and then either incubated at 4 °C for surface detection or incubated at 37 °C for 1 h to allow internalization. When indicated, 1 μM PMA was added during the 37 °C incubation. To get a measure of internalized protein, the fraction of M1 still present at the surface after the 37 °C incubation was stripped off using acid buffer. Internalization is expressed relative to the initial surface signal (4 °C). Means ± S.E. of $n = 3–6$, *, $p < 0.05$; ***, $p < 0.001$ one-way ANOVA, Dunnett's post-test.

cell surface (19). Earlier, we have made a similar construct for DAT, TacDAT, which was used to study DAT trafficking (17).

To establish whether SERT is constitutively internalized, as shown previously for DAT (12, 16, 17), TacSERT was transiently expressed in CAD cells, a neuronal cell line, and an antibody-based internalization assay was performed. As a negative control, the FLAG-tagged single transmembrane protein Tac (Tac) was assayed in parallel. CAD cells expressing TacSERT or Tac were labeled with Alexa568-conjugated M1 antibody at 4 °C where internalization is blocked. Subsequently, internalization was allowed by incubating cells at 37 °C for 30 min. Confocal microscopy analysis showed a clear intracellular accumulation of the M1 antibody in cells expressing TacSERT, indicating that TacSERT is indeed constitutively internalized during the 30-min incubation (Fig. 1*B*). No apparent internalization was observed when the cells expressing TacSERT were kept at 4 °C (Fig. 1*B*). In contrast, Tac was only found at the surface independently of incubation temperature indicating that Tac alone resides in the plasma membrane and does not internalize to a detectable extent during the 30-min incubation time (Fig. 1*B*). The experiments were also performed in HEK293 cells showing a similar intracellular accumulation of TacSERT upon incubation with the M1 antibody for 30 min at 37 °C (data not shown).

Stimulation with PMA has previously been shown to internalize SERT. To verify that TacSERT expressed in CAD cells retained the trafficking properties observed for the wild type transporter, we performed the antibody feeding internalization assay with 1 μM PMA in the cell media. The presence of PMA during the internalization period substantially increased the amount of intracellularly accumulated TacSERT (Fig. 1*B*), indicating that TacSERT is subject to PMA-induced internalization in CAD cells as observed for wild type SERT in other cell systems (6, 25, 26). Still no visible intracellular accumulation of M1 was observed for Tac alone (Fig. 1*B*).

To quantify the amount of internalized SERT, we used an ELISA-based internalization assay (for schematic overview of the assay, see Ref. 17). CAD cells transiently transfected with TacSERT were incubated with M1 antibody at 4 °C to label surface transporter. Next, constitutive internalization was allowed by incubating cells at 37 °C for 45 min. Surface-bound M1 was removed by an acid strip; cells were permeabilized, and intracellular accumulated transporter was measured by ELISA. Internalization was calculated as the fraction of intracellular accumulated TacSERT relative to the initial surface expression (Fig. 1*C*). Using the same assay, our group has previously shown that the Tac-tagged version of the DAT, TacDAT, is constitutively internalized, whereas only very limited internalization is seen for Tac alone (17). Accordingly, TacDAT and Tac alone were included for comparison. TacSERT was constitutively internalized to the same extent as TacDAT (intracellular accumulation of 9.8 ± 3.0 and 9.9 ± 1.3%, respectively). Furthermore, both the fractions of internalized TacSERT and TacDAT were significantly different from the negative control Tac (4.2 ± 0.61%) (Fig. 1*C*). In addition, it was tested whether incubation with PMA increased intracellular accumulation of TacSERT. In concordance with the microscopy data in Fig. 1*B*, PMA significantly increased the amount of internalized transporter (19.8 ± 0.95%) and had no effect on the negative control Tac (4.6 ± 0.66%) (Fig. 1*C*).

SERT Internalization Is Dynamin-dependent—To investigate the mechanism underlying constitutive internalization of SERT, we examined whether the process is dynamin-dependent. TacSERT was co-expressed in CAD cells with either wild type (WT) dynamin I or the dominant negative dynamin I (K44A) (27), and constitutive internalization was measured in the ELISA-based internalization assay as described above. In cells transfected with TacSERT and WT dynamin I, internalization of TacSERT was observed to the same extent as when TacSERT was co-transfected with the empty pcDNA3.1 vector (Fig. 2*A*). However, constitutive internalization was significantly reduced when cells were transfected with the dominant negative dynamin I (Fig. 2*A*). We also performed the immunofluorescence antibody feeding assay on CAD cells co-expressing TacSERT and either EGFP-tagged WT dynamin I or negative dynamin I K44A. Expression of EGFP-tagged versions of dynamin I enabled detection of TacSERT trafficking in only EGFP-dynamin I positive transfected cells. As observed in cells expressing TacSERT alone, M1 antibody accumulated intracellularly in EGFP-dynamin I-expressing cells in agreement with internalization of TacSERT. However, accumulation of M1 antibody and thereby TacSERT internalization was impaired in EGFP-dynamin I K44A-positive cells (Fig. 2*B*). Together, the results support that TacSERT undergoes constitutive endocy-

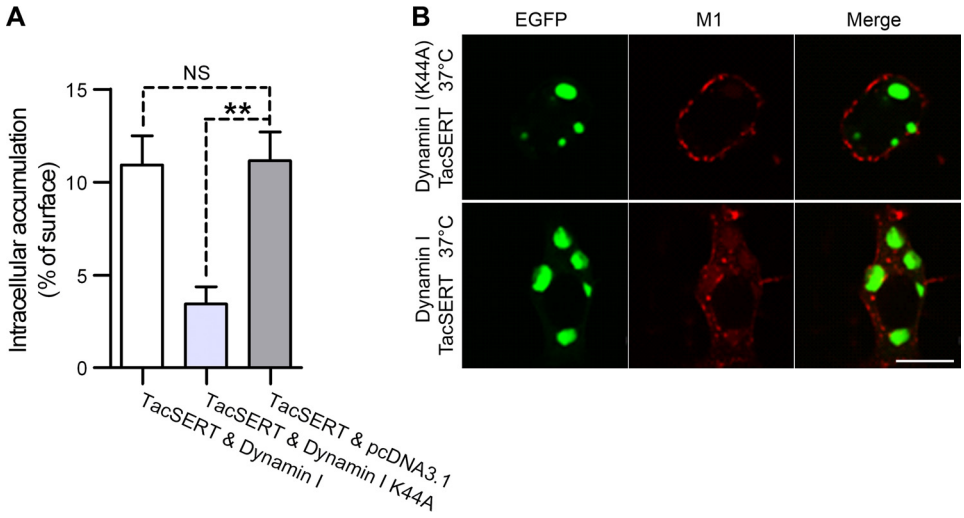

FIGURE 2. **Constitutive internalization of SERT is dynamin-dependent.** CAD cells were co-transfected with TacSERT and wild type dynamin I, dominant negative (K44A) dynamin I, or the empty vector pcDNA3.1. *A*, intracellular accumulation of TacSERT measured in the ELISA-based internalization assay. *NS* is not significant. Values represent the mean ± S.E. of $n = 3$, **, $p < 0.01$; two-way ANOVA. *B*, immunofluorescence-based internalization assay. Confocal images of cells after 60 min of Alexa568 M1-conjugated antibody internalization. Data are representative of at least three independent experiments. *Scale bar,* 10 μm.

tosis and that this endocytosis occurs through a dynamin I-dependent pathway.

Characterization of the Postendocytic Sorting of Internalized SERT—To determine the fate of internalized SERT, we took advantage of EGFP-fused Rab proteins. Rab proteins are small GTPases that play an important role in regulating intracellular trafficking pathways (28). As trafficking regulators, each Rab-GTPase has a distinct intracellular localization and function. Consequently, the Rab-GTPases can be used as intracellular markers. Rab4 is a marker of early endosomes as well as the so-called short loop recycling pathway, whereas Rab11 is a marker of recycling endosomes associated with the long loop recycling pathway. Rab7, however, associates with late endosomes/lysosomes (28, 29). The immunofluorescence antibody feeding assay was applied in CAD cells co-expressing the various EGFP-Rabs and TacSERT (Fig. 3*A*). The confocal microscopy images showed that internalized TacSERT was distributed rather differently than EGFP-Rab4, although partially overlapping signals were observed in some parts of the cells (Fig. 3*A*). A more profound co-localization was observed between TacSERT and Rab7, the marker of late endosomes/lysosomes, *i.e.* the distribution was remarkably similar for EGFP-Rab7 and internalized TacSERT, and characterized by multiple overlapping vesicular structures (Fig. 3*A*). In contrast, we saw only little overlap between the TacSERT immunosignal and the signal from EGFP-Rab11 (Fig. 3*A*). Quantifications of overlapping M1 TacSERT signal and Rab EGFP signal supported these observations and showed significantly higher co-localization of TacSERT with EGFP-Rab7 and EGFP-Rab4 than with EGFP-Rab11 (Fig. 3*B*).

As a control for the co-localization assay, we included an N-terminally FLAG-tagged β_2-AR in our experiments. β_2-AR is known to undergo endocytosis and subsequent recycling upon stimulation with the agonist isoproterenol. When co-expressing FLAG-tagged β_2-AR with the various EGFP-Rabs in CAD cells, we found a pronounced co-localization of the immunosignal from isoproterenol-internalized β_2-AR with the signal from EGFP-Rab11 (Fig. 3*C*). In further contrast to our findings for TacSERT, there was almost no co-localization between the β_2-AR immunosignal and the EGFP-Rab7 signal. However, as for TacSERT, the β_2-AR immunosignal and the EGFP-Rab4 signal distributed rather differently in the cells, although an overlapping signal was seen in certain parts of the cell. Quantifications of co-localized β_2-AR with EGFP-tagged Rab proteins confirmed these findings with a significant sorting to EGFP-Rab4 and EGFP-Rab11 positive compartments compared with EGFP-Rab7 positive compartments (Fig. 3*D*). This sorting pattern of β_2-AR is in accordance with previous published data (17, 30, 31).

To further assess the postendocytic fate of SERT, we used LysoTracker, a commercially available fluorescently labeled marker of lysosomes, or Tf-488 (Alexa Fluor 488-conjugated transferrin), a marker of early endosomes and recycling endosomes, in the M1 feeding internalization assay. Tf-488 labels endogenously expressed transferrin receptors, which are internalized into early endosomes and subsequently sorted to recycling endosomes. Corresponding to the observations made when the Rab-GTPases were used as markers, only a very limited fraction of the transporter that internalized over 30 min showed co-localization with the signal from Tf-488 (Fig. 4*A*). However, in the same assay, a prominent overlap of TacSERT with LysoTracker was found with a large fraction of the intracellular vesicles showing both M1 immunosignal and LysoTracker signal (Fig. 4*B*). Quantifying the co-localization of TacSERT with either LysoTracker or Tf-488 showed a highly significant difference in co-localization between the two markers (Fig. 4*C*). For the β_2-AR, a prominent co-localization with Tf-488 was observed and to a lesser extent co-localization with LysoTracker (data not shown).

Finally, we applied the cation ionophore monensin, which is a blocker of both lysosomal degradation and recycling (32). If a major fraction of SERT is targeted to recycling, a decrease in the steady state SERT surface level would be expected upon treatment with monensin. Accordingly, CAD cells expressing

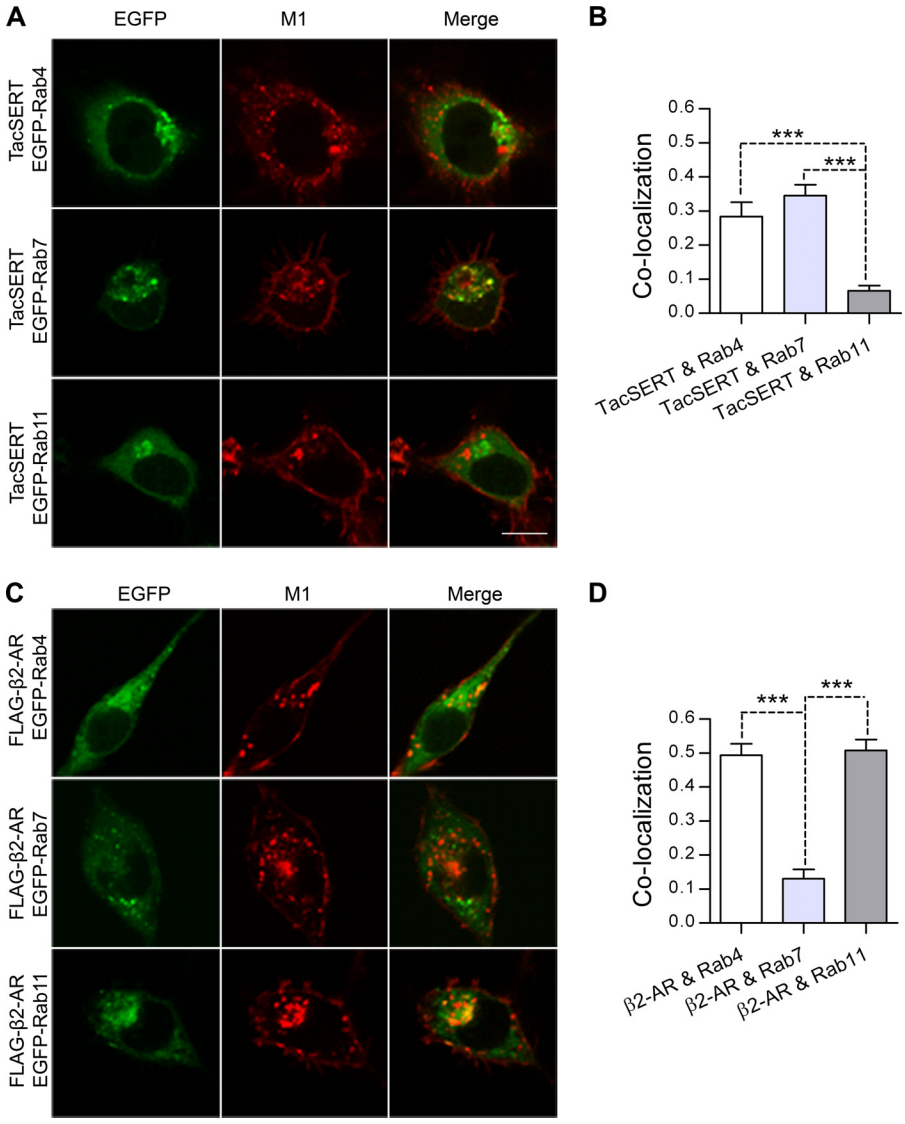

FIGURE 3. **SERT co-localizes with the late endosomal marker Rab7.** Confocal microscopy images obtained after 30 min of Alexa568 M1-conjugated antibody internalization, showing putative co-localization between internalized TacSERT (*A*) or FLAG-tagged β_2-AR (*C*) and EGFP-tagged Rab4, Rab7, or Rab11 co-expressed in CAD cells. For the cells expressing β_2-AR, 10 μM isoproterenol was included during the internalization. *Scale bar,* 10 μm. *B* and *D*, quantifications of co-localizations in *A* and *B* between internalized TacSERT (*B*) or internalized β_2-AR (*D*) and the EGFP-tagged Rab4, Rab7, or Rab11 (means ± S.E. ***, $p < 0.001$, one-way ANOVA, Bonferroni's multiple comparison test). Data were analyzed from 25 to 35 images of each condition from three independent experiments.

TacSERT, Tac alone, or the β_2-AR were treated with 25 μM monensin for 1 h before surface levels were measured by ELISA. As shown in Fig. 4*D*, no significant effect of monensin was observed for TacSERT surface levels, although agonist-stimulated β_2-AR receptors (included as a positive control) were sensitive to the treatment (Fig. 4*D*).

Postendocytic Sorting of SERT Following PMA Stimulation—It is well established that phorbol esters, *i.e.* PMA, which activate kinases such as PKC, cause acute internalization of SERT (6, 7). However, the postendocytic fate of PMA-induced internalization of SERT has never been investigated. To shed light on this matter, we first confirmed that stimulation with PMA leads to an increase in intracellular SERT in CAD cells using the M1-based internalization assay (Fig. 1*B*). Next, postendocytic sorting of TacSERT in the presence of PMA was assessed. CAD cells were co-incubated with the marker of recycling, Tf-488, and the lysosomal marker, LysoTracker, as described above. As observed upon constitutive internalization, M1-labeled TacSERT showed only little co-localization with Tf-488, whereas a clear overlap with LysoTracker was observed (Fig. 5*A*). When employing the EGFP-tagged Rab proteins, we also saw the same sorting pattern as that seen upon constitutive internalization. As shown in Fig. 5*B*, TacSERT internalized in response to PMA was predominantly found to co-localize with EGFP-Rab7 and not with EGFP-Rab11 (Fig. 5*B*), indicating that SERT is primarily destined for lysosomal degradation following both constitutive and PMA-stimulated internalization.

HA-tagged SERT Is Also Sorted to Rab7/LysoTracker-positive Compartments—The data presented so far rely on the TacSERT construct in which the N terminus is tethered by the addition of an extra transmembrane segment. The fusion of Tac to SERT made it possible to tag the transporter with the FLAG tag at the extracellular part of the transporter; however, tethering of the N terminus could potentially affect the trafficking properties of

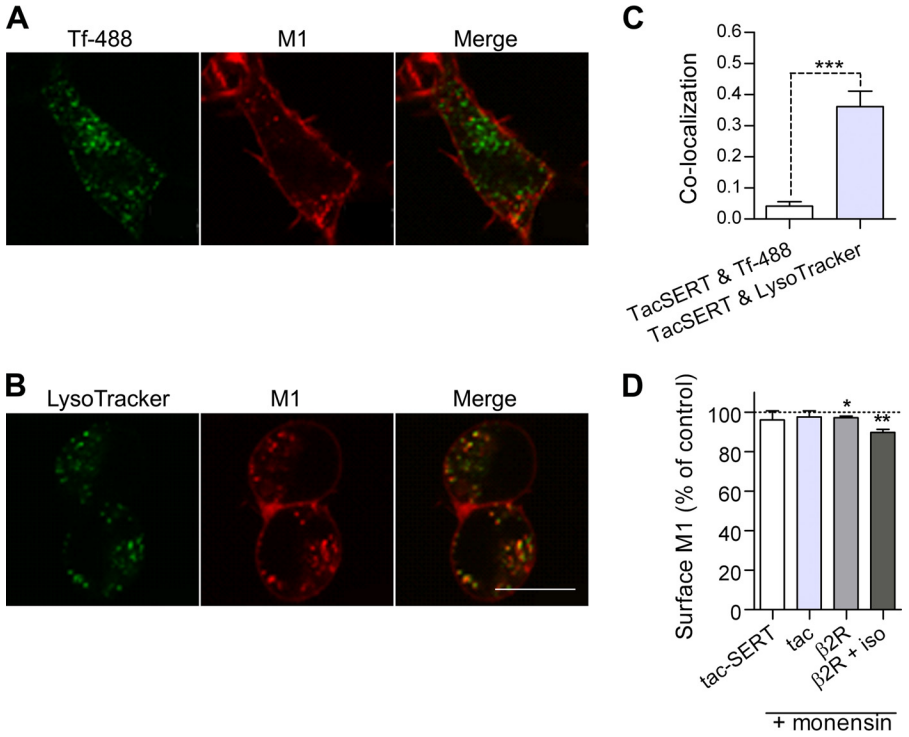

FIGURE 4. **SERT co-localizes with the lysosomal marker LysoTracker.** Confocal microscopy images of internalized TacSERT and Tf-488 (*A*) or LysoTracker Green (*B*) after 30 min of Alexa568 M1-conjugated antibody internalization in the presence of Tf 488 or LysoTracker. *Scale bar,* 10 μm. *C*, quantifications of co-localizations in *A* and *C* between internalized TacSERT and Tf-488 or LysoTracker Green (means ± S.E. of $n = 3$, ***, $p < 0.001$, one-way ANOVA, Bonferroni's multiple comparison test). Data were analyzed from 25 to 35 images of each condition. *D*, surface ELISA in CAD cells expressing TacSERT, Tac, or β_2-AR after 1 h treatment with monensin (25 μM). Isoproterenol (*iso*) was included when indicated during monensin treatment (means ± S.E. of $n = 4–5$, *, $p < 0.05$; **, $p < 0.01$, paired *t* test).

SERT. Interestingly, Sorkin et *al.* (33) succeeded in introducing the hemagglutinin (HA) epitope tag (YPYDVPDYASL) in the second extracellular loop (EL2) of the closely related DAT without perturbing transporter function and expression. Accordingly, we introduced the HA tag between the two glycosylation sites in EL2 of SERT (Fig. 6*A*). The resulting construct, HA-SERT, was expressed transiently in CAD cells, and 5-[^{3}H]HT uptake activity was compared directly with WT SERT. The V_{max} value for HA-SERT was 55.0 ± 7.0% (mean ± S.E., $n = 3$) of WT SERT, and the K_m value of HA-SERT (0.82 ± 0.07 μM) was comparable with the K_m value observed for the wild type SERT (0.57 ± 0.05 μM) (mean ± S.E., $n = 3$). A representative graph of the kinetic measurements of 5-[^{3}H]HT uptake in CAD cells expressing wild type or HA-SERT is shown in Fig. 6*B*. Introducing the HA tag in any other position in EL2 than between the two glycosylation sites led to a complete loss of function in the uptake assay (data not shown).

It has been shown previously that the HA.11 antibody binds poorly to the HA-tagged DAT at 4 °C (33). Accordingly, to label transporters at the cell surface, CAD cells expressing HA-SERT were incubated with Alexa568-conjugated HA.11 at 18 °C, conditions of minimal or no endocytosis. Without a subsequent incubation at 37 °C to allow internalization, the HA antibody was clearly detected at the cell surface (Fig. 6*C*), confirming that the HA epitope is exposed to the extracellular side of the membrane and that the transporter protein is indeed expressed at the surface of the cell. Allowing internalization of labeled surface transporters for 30 min at 37 °C resulted in a distinct intracellular accumulation of labeled HA-SERT in accordance to the results obtained for cells expressing TacSERT. Likewise, a further increase in intracellular HA-SERT was observed when 1 μM PMA was included in the media during the 37 °C incubation (Fig. 6*C*). Taken together, these data suggest that HA-SERT can be used reliably to study SERT trafficking.

Next, we tested whether constitutive endocytosis of HA-SERT was dynamin-dependent as observed for TacSERT. CAD cells were co-transfected with HA-SERT and dynamin I or dynamin I K44A, and intracellular accumulation of transporter was assessed by HA.11 antibody feeding. Intracellular accumulation of the HA.11 immunosignal was markedly impaired in cells co-expressing the dominant negative dynamin I K44A but not in cells expressing the WT dynamin I (Fig. 7*A*). Finally, the co-localization of internalized HA-SERT with the various EGFP-tagged Rab proteins as well as with LysoTracker or Tf-488 was imaged and quantified as described above for TacSERT. The quantifications are depicted in Fig. 7*B* and confirm that the highest degree of co-localization is observed between HA-SERT and the markers of late endosomes and lysosomes (Rab7 and LysoTracker). An overlap was also observed with EGFP-Rab4 similar to our findings for TacSERT, whereas little overlap was seen between HA-SERT and the marker of the long loop recycling pathway. We also found little overlap between the HA-SERT immunosignal and the transferrin signal (Tf-488) (Fig. 7*B*).

Internalized hSERT Distributes Mainly to Rab7-positive Compartments in an Antibody-independent Assay—To exclude that sorting of internalized SERT was influenced by the bound antibody, we wanted to test the postendocytic fate of the trans-

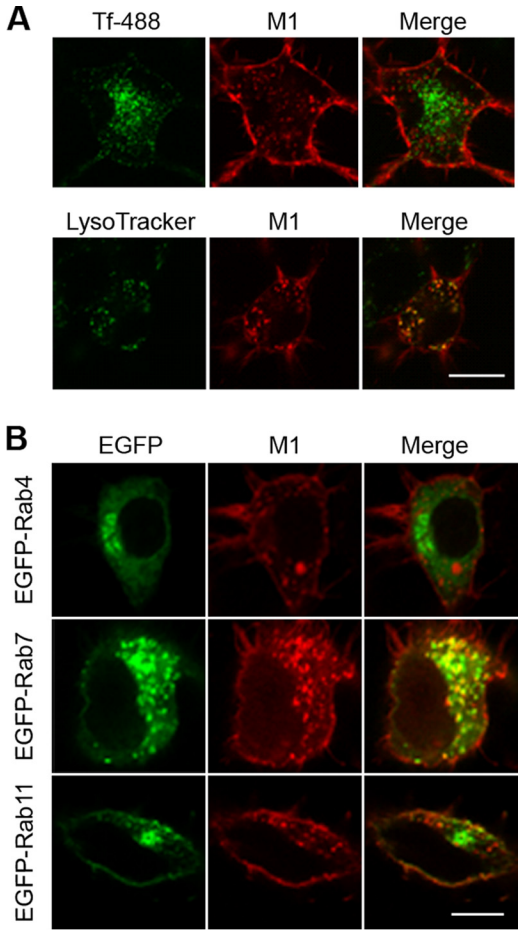

FIGURE 5. **Postendocytic sorting of TacSERT after PMA stimulation.** Confocal microscopy images of co-localization between internalized TacSERT and Tf-488 or LysoTracker Green (*A*) or EGFP-tagged Rab proteins (*B*) after 30 min of Alexa568 M1-conjugated antibody internalization in the presence of 1 μM PMA are shown. Tf-488 or LysoTracker was added to the media during time of internalization. Images are representative of three independent experiments. *Scale bar,* 10 μm.

porter in an antibody-independent assay. The fluorescent cocaine analog JHC1-64 has previously been shown to inhibit uptake in SERT, the norepinephrine transporter, and DAT (18); JHC1-64 has also been used to demonstrate internalization of DAT in CAD cells, as well as in dopaminergic neurons, and importantly, the compound did not affect trafficking of the transporter *per se* (10, 17). To support previous findings that the fluorescent cocaine analog JHC1-64 labels and visualizes transiently expressed SERT in the nanomolar range (19, 34), we incubated CAD cells transiently expressing SERT tagged at the N terminus with EGFP (EGFP-SERT) with 10 nM JHC1-64 alone or together with 1 μM paroxetine, a SERT-specific blocker. Confocal live imaging of the cells showed clear EGFP fluorescence corresponding to the plasma membrane of a subset of cells, conceivably corresponding to the cells transfected with EGFP-SERT. Importantly, there was strong JHC1-64 plasma membrane labeling of the same cells, and this labeling was eliminated in the presence of an excess of paroxetine (Fig. 8).

Next, we transfected CAD cells with untagged hSERT together with EGFP-Rab4, -7 or -11. To assess whether hSERT internalization could be detected with JHC1-64, the cells were incubated first at 15 °C with 20 nM JHC1-64 resulting in plasma membrane labeling without any signs of intracellular accumulation of the fluorophore (Fig. 9). This supports that the compound does not penetrate the cell membrane in a nonspecific manner. Raising the temperature to 37 °C, and thus to a trafficking-permissive temperature, led to the appearance of JHC1-64-positive intracellular vesicular structures, supporting internalization of the JHC1-64·SERT complex (Fig. 9). Notably, the JHC1-64-positive vesicles almost exclusively co-localized with Rab7- and only few vesicles overlapped with Rab4 and Rab11 (Fig. 9), in agreement with our observations using either TacSERT or HA-SERT.

Assessing Internalization by Reversible and Pulse-Chase Biotinylation—To investigate internalization and the fate of internalized SERT by an approach independent of fluorescence imaging, we first utilized a reversible biotinylation strategy. CAD cells were transiently transfected with SERT tagged at the N terminus with a short c-Myc epitope, which does not affect expression and function of SERT (38). Cells were biotinylated with the reducible biotinylation reagent, sulfo-NHS-S-S-biotin, containing a cleavable disulfide bond, and subsequently internalization was allowed by incubation of the cells at 37 °C for 2 h. Surface biotin was removed by treating cells with a reducing agent (2-mercaptoethanesulfonic acid (MesNa)), and intracellular biotinylated protein was isolated from the lysed cells with avidin beads, followed by SDS-PAGE and immunoblotting. A noninternalized (ice), unstripped sample and a noninternalized (ice), stripped sample ("strip" control) defined total SERT at the cell surface and the stripping efficiency (93–96%) of the assay (Fig. 10*A*). In agreement with our antibody feeding assays, the data provided evidence for constitutive SERT internalization, *i.e.* SERT immunoreactivity was markedly stronger for cells incubated at 37 °C compared with cells kept on ice (strip control) (Fig. 10*A*). To assess whether internalized SERT underwent lysosomal degradation during the incubation period, we incubated cells with the lysosomal protease inhibitor, leupeptin, either alone or together with the lysosomotropic agent chloroquine (35). In the presence of leupeptin and chloroquine, we observed a significant increase in SERT immunoreactivity, supporting that a detectable fraction of internalized SERT was targeted to degradation during the incubation period (Fig. 10*A*). Of note, the reversible biotinylation protocol permitted calculations of the cumulated fraction of internalized SERT (internalized relative to unstripped control), which was 13.5 ± 2.8% in the presence of leupeptin and chloroquine, 9.88 ± 2.2% in the presence of leupeptin, and 7.61 ± 2.1% without leupeptin and chloroquine (means ± S.E., $n = 4$).

Finally, we incubated the cells with both leupeptin and the recycling inhibitor monensin (17). This treatment did not cause any significant increase in SERT immunoreactivity as compared with leupeptin alone or leupeptin and chloroquine together, arguing against that a major fraction of internalized SERT undergoes recycling during the 2 h incubation period.

To obtain additional evidence that a significant fraction of internalized SERT is targeted to lysosomal degradation, we performed a "pulse-chase" biotinylation experiment using a nonreducible biotinylation reagent. Unfortunately, despite several attempts and optimization procedures, we were unable to per-

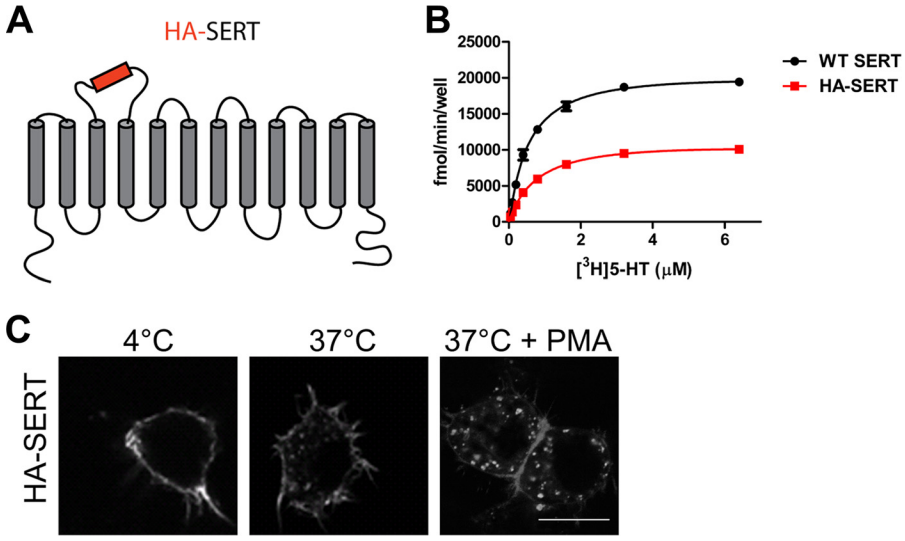

FIGURE 6. **HA-tagged SERT expressed at the cell membrane is functional and is internalized constitutively and after PMA treatment.** *A*, topology diagram of HA-SERT with the HA epitope inserted in the EL2. *B*, kinetic measurements of specific 5-[^{3}H]HT uptake in CAD cells expressing WT SERT (K_m, 0.587 μM; V_{max}, 21,771 fmol/min/well) or HA-SERT (K_m, 0.727 μM; V_{max}, 11,430 fmol/min/well). The *curve* is representative of three independent experiments. *C*, antibody feeding internalization assay. Confocal images of CAD cells expressing HA-SERT detected by Alexa568-conjugated HA.11. After incubation with the antibody at 18 °C, cells were either kept at 4 °C (no trafficking) or at 37 °C for 30 min to allow internalization. When indicated, 1 μM PMA was added during the 37 °C incubation. *Scale bar*, 10 μm.

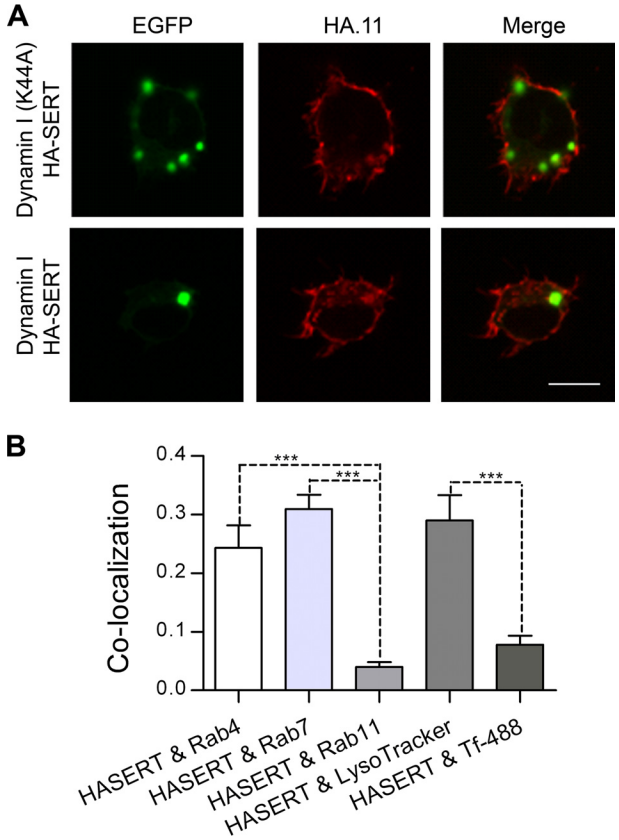

FIGURE 7. **HA-SERT is internalized via a dynamin I-dependent pathway and co-localizes with Rab4 and Rab7.** *A*, CAD cells co-transfected with HA-SERT and wild type dynamin I, dominant negative (K44A) dynamin I, or the empty vector pcDNA3.1. *B*, quantifications of co-localizations between internalized HA-SERT and EGFP-tagged Rab4, Rab7, or Rab11 or LysoTracker or Tf-488 (means ± S.E., ***, $p < 0.001$, one-way ANOVA, Bonferroni's multiple comparison test). Data were analyzed from 25 to 35 images of each condition from three independent experiments.

form the experiment on CAD cells because these cells did not stick sufficiently well to the surface during the required 4-h incubation period. We therefore turned to HEK293 cells, which did not show the same problem. Importantly, constitutively internalized SERT sorted similarly in HEK293 cells as in CAD cells. In HEK293 cells transiently expressing SERT, together with either Rab4, -7 or -11, we carried out an internalization assay using the fluorescent cocaine analog JHC1-64. As in the CAD cells, the internalized JHC1-64-positive vesicles primarily co-localized with Rab7 and only to a small extent with Rab4 and Rab11 (data not shown). For the pulse-chase experiment, surface SERT was labeled with nonreducible sulfo-NHS-biotin on ice and subsequently allowed to internalize for 4 h at 37 °C with and without the lysosomal protease inhibitor leupeptin. The biotin-linked SERT remaining after the incubation was bound to streptavidin beads and quantified using SDS-PAGE and immunoblotting (Fig. 10*B*). The two samples (± leupeptin) were normalized to a third sample (total surface) collected after biotinylation, prior to internalization. The signal detected should reflect the remaining biotin-linked SERT after 4 h, independent of which intracellular compartment the biotin-linked SERT may reside. If a fraction of the protein has undergone lysosomal degradation, we would expect a smaller loss in the leupeptin-treated sample compared with vehicle. Indeed, we observed a significantly lower loss in the presence of leupeptin equivalent to 0.11%/min loss of protein over 4 h compared with 0.18%/min loss of protein for the vehicle-treated sample (Fig. 10*B*).

DISCUSSION

It is well established that the level of SERT protein at the plasma membrane is subject to tight control by a series of different kinases and interacting proteins. However, whether SERT undergoes constitutive internalization *per se* has not previously been addressed. Furthermore, to the best of our knowledge, no previous study has addressed the postendocytic fate of internalized SERT, although such information should be critical for understanding the mechanisms controlling the level and activity of SERT in the presynaptic membrane. A major reason

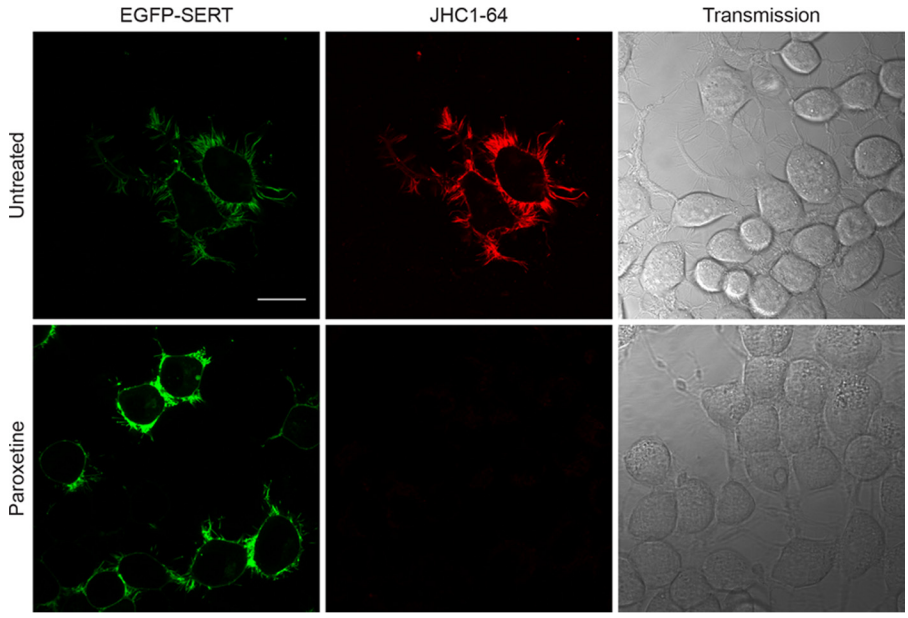

FIGURE 8. **JHC1-64 binds specifically to SERT.** Confocal microscopy images of co-localization between EGFP-SERT were transiently expressed in CAD and the fluorescent cocaine analog JHC1-64. Images were taken after 10 min of incubation with 10 nM JHC1-64 alone or together with 1 μM of the SERT-specific antagonist paroxetine. Cells treated with paroxetine were preincubated for 10 min before the addition of JHC1-64. Data are representative of three independent experiments. *Scale bar,* 20 μm.

for this lack of knowledge is the challenge of studying SERT trafficking because of difficulties in developing an efficient antibody against an endogenous extracellular epitope of the transporter.

This study was made possible by the introduction in SERT of extracellular FLAG or HA tags, enabling the use of commercially available high affinity antibodies. The FLAG-tagged TacSERT was generated by fusion of the one transmembrane protein Tac to the N terminus of SERT. Tac appears essentially inert in its trafficking properties and has been used ubiquitously to reveal, for example, endocytosis motifs in other membrane proteins by chimeric fusion of selected sequences to its C terminus (36, 37). In agreement with previous published data for WT SERT, TacSERT was expressed at the cell surface and was shown to internalize in response to PMA stimulation (Fig. 1*B*). The V_{max} and K_m values for 5-HT uptake in TacSERT were likewise equivalent to that of SERT (19). Of note, we showed previously that the corresponding TacDAT construct also has preserved uptake properties and, moreover, that it retains the trafficking properties of wild type DAT (17). Inspired by the work of Sorkin *et al.* (33) on DAT, we also generated a SERT with an HA tag in EL2. This construct was functional and expressed at the cell surface, although V_{max} for 5-HT uptake was reduced by around 50% (Fig. 6*C*). Possibly, this reduction is the result of a structural perturbation caused by inserting the HA sequence between the two glycosylation sites in the EL2. Indeed, we know from previous studies that mutations interfering with glycosylation in EL2 of SERT alter transporter protein expression (38).

TacSERT and HA-SERT have each their own advantages. TacSERT possesses the advantage over HA-SERT that the M1 signal is almost 10-fold higher than the corresponding HA signal in the quantitative ELISA, improving the signal to noise ratio considerably (17). Furthermore, binding of the antibody to Tac, rather than to the transporter itself, makes interference from antibody binding on the trafficking properties of the transporter less likely. However, tethering of the N terminus as in TacSERT might interfere with function as indicated by the previously shown altered capacity to mediate amphetamine-induced efflux for this construct (19). It was therefore highly important that both constructs were suitable for the immunocytochemistry-based antibody feeding internalization assay. It was also very important that we observed the same internalization and postendocytic sorting properties for the two different constructs, strongly supporting that our observations are not a consequence of alterations made by introduction of the epitope tags.

Using the antibody-feeding internalization assay in the neuronal cell line, CAD, expressing TacSERT or HA-SERT, we show that the transporter is constitutively internalized to an extent that is significantly higher than that of the control membrane protein Tac (Figs. 1*B* and 6*C*). This finding was confirmed in a quantitative ELISA-based internalization assay in cells expressing TacSERT (Fig. 1*C*). In further support of an endocytic event is the finding that the process is dynamin-dependent (Fig. 2). Of note, we also attempted to block internalization with specific dynamine inhibitors, such as Dynasore, Dyngo4a, and Dynole; however, in our hands, these compounds caused a dramatic loss in signal, often accompanied by cell detachment, making our experiments inconclusive.

To further substantiate our observations and exclude that antibody binding, or the tags themselves, affected the trafficking properties of TacSERT and HA-SERT, we took advantage of the rhodamine-conjugated cocaine analog JHC1-64 and a reversible biotinylation protocol. We have previously used JHC1-64 to demonstrate internalization of DAT (17). Here, we show that the compound can be used to demonstrate internalization of untagged human SERT as well. Our reversible bioti-

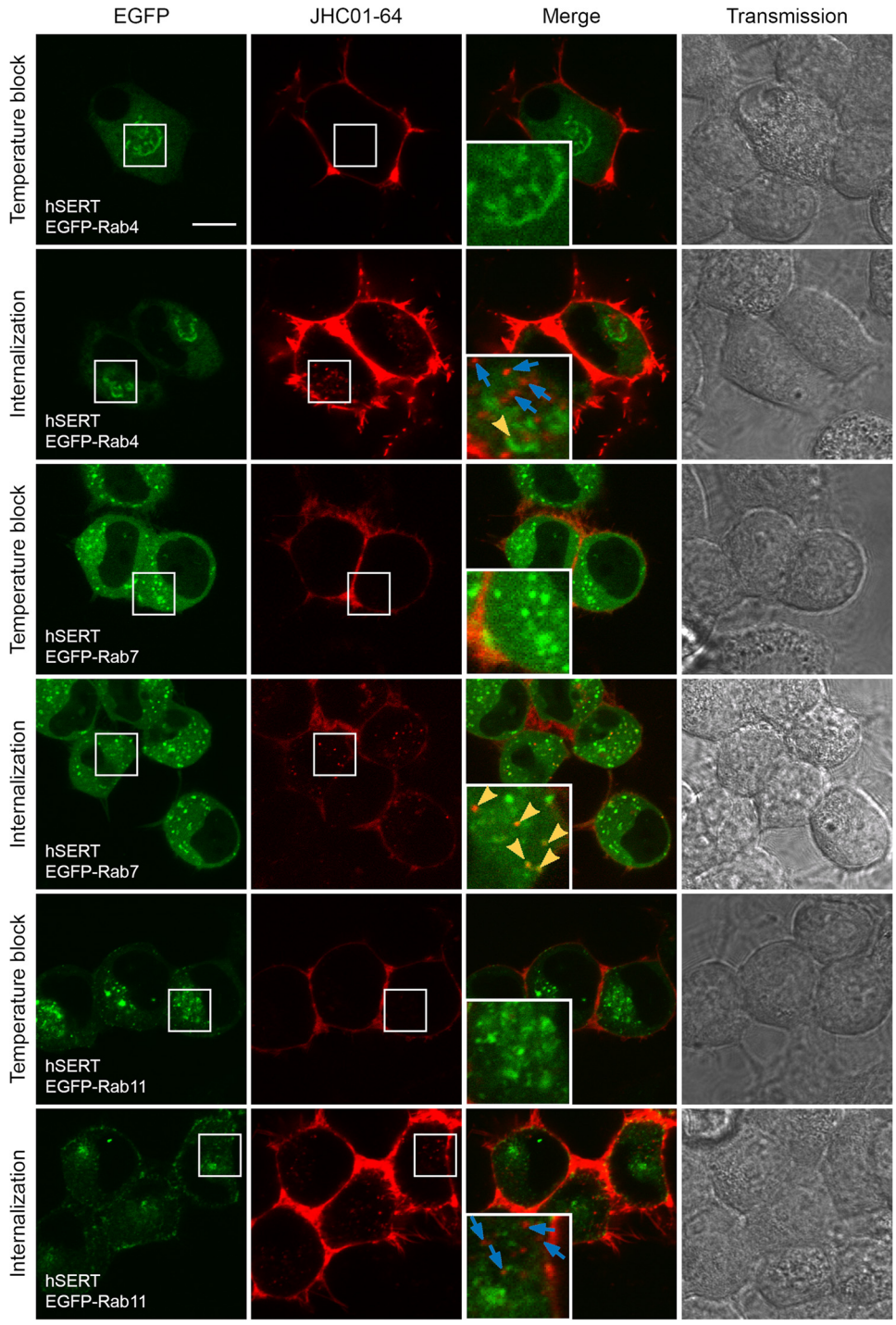

FIGURE 9. **Internalized JHC1-64 labeled hSERT co-localizes with the late endosomal marker Rab7.** Confocal microscopy images of co-localization between hSERT, visualized by JHC1-64, and EGFP-tagged Rab4, Rab7, or Rab11 co-expressed in CAD cells. For the temperature block, images were taken after 30 min at 15 °C with 20 nM JHC1-64 and three washes. For internalization, images were taken after 30 min at 15 °C with 20 nM JHC1-64 and two washes prior to 1 h of internalization in cell media at 37 °C and two washes. *Blue arrows* indicate JHC1-64-positive vesicles that show no co-localization with EGFP. *Yellow arrowheads* indicate areas of co-localization between JHC1-64-positive vesicles and EGFP. Data are representative of 3–4 independent experiments. *Scale bar,* 10 μm.

nylation also revealed constitutive trafficking of SERT, directly supporting our observations with TacSERT, HA-SERT, and JHC1-64. Of interest, the reversible biotinylation protocol permitted, in addition, another way of quantifying constitutive trafficking.

Our calculations revealed an apparent fractional internalization over 2 h of ~13.5% in the presence of leupeptin and chloroquine and ~8% in the absence of these compounds. The fractional internalization estimated from the ELISA internalization assay was slightly lower (~10% over 1 h), a difference that probably can be attributed to the different methodological approaches. The ELISA internalization assay also revealed a fractional internalization of the transporter in the presence of PMA, which amounted to ~20% over 1 h. This might seem low

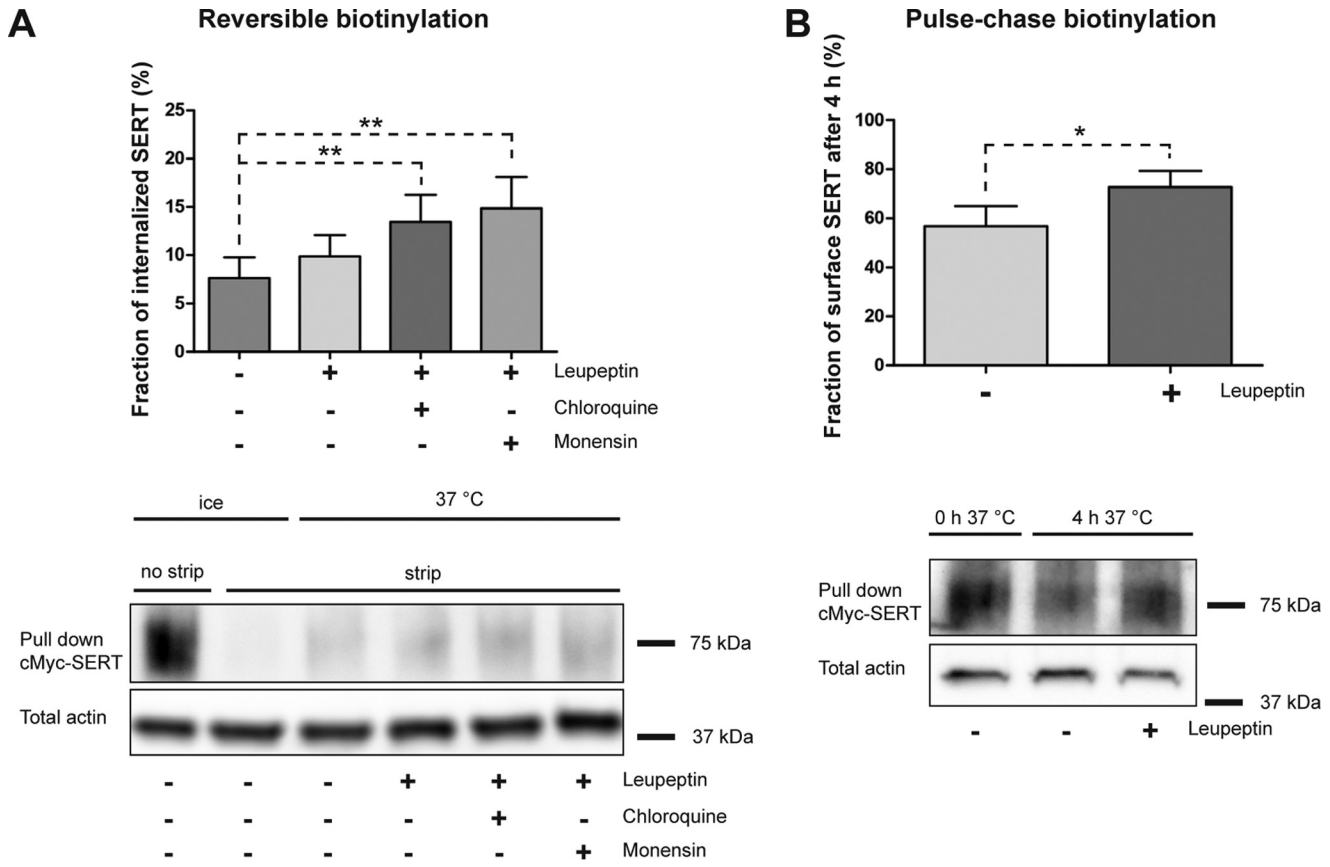

FIGURE 10. **Blocking proteases and recycling increases the intracellular pool of constitutively internalized c-Myc-SERT.** *A*, reversible biotinylation assay on transiently expressed c-Myc-SERT in CAD cells. c-Myc-SERT was allowed to internalize for 2 h at 37 °C while incubated with no extra treatment, 10 μg/ml leupeptin, 10 μg/ml leupeptin + 200 μM chloroquine, or 10 μg/ml leupeptin + 25 μM monensin, before stripping the surface biotin. Stripping efficiency was 93–96%. Biotinylated protein was analyzed by SDS-PAGE followed by immunoblotting. A representative blot (representative of five independent experiments) is shown in the *lower panel,* and quantification of the data is shown in the *upper panel*. The background immunosignal seen in the strip control (ice plus strip) was subtracted from the immunosignal of the internalized samples before normalization. Data are means ± S.E., **, $p < 0.01$, one-way ANOVA, Bonferroni's multiple comparison test, $n = 5$. *B*, pulse-chase biotinylation assay on c-Myc-SERT in HEK293 cells. c-Myc-SERT was biotinylated with a nonreducible biotin and allowed to internalize for 4 h ± 100 μg/ml leupeptin. Remaining biotinylated protein was analyzed by SDS-PAGE followed by immunoblotting. The experiment shown (*lower panel*) is representative of five independent experiments, and quantification of the data is shown in the *upper panel*. Quantification of the remaining SERT was normalized to a third sample lysed before internalization. Data are means ± S.E. *, $p < 0.05$, *t* test, $n = 5$.

compared with previous studies investigating PMA-induced SERT internalization. For example, ~70% loss of surface SERT over 30 min has been observed in platelets (25) and ~50% loss over 30 min in transfected HEK293 cells (39). However, ~40% reduction over 40 min was seen in transfected HEK293 cells (6) and ~30% reduction over 30 min in brain synaptosomes (26), and 14% reduction was seen over 2 h in JAR human placental choriocarcinoma cells (40). Thus, internalization rates are likely to differ quite substantially between different cellular systems and different experimental approaches. We have no immediate explanation for the relatively low rates seen in this study other than it most likely relates to the cells used and the methods applied. It is important to note, however, that the actual internalization might be higher than indicated from the biotinylation experiments if leupeptin and/or chloroquine did not completely block lysosomal degradation during the incubation periods used. However, we find it less likely that we have a loss of signal because of spontaneous disulfide reduction of the biotinylation reagent in the reversible biotinylation experiment. In contrast to the reducing environment of the cytosol, the endosomal environment, to which the surface biotinylated SERT is exposed, is believed to be oxidative (41).

A marked constitutive internalization has also been shown for other members of the SLC6 transporter family such as the DAT, GLYT2, and norepinephrine transporter (11, 12, 42). However, the fate of constitutively internalized SLC6 transporters, and ultimately the consequences of the internalization, remains elusive. To investigate the fate of internalized SERT, we took advantage of Rab proteins fused to EGFP in combination with confocal imaging. In CAD cells, by co-expression of TacSERT with the EGFP-tagged Rab proteins, we observed the most pronounced co-localization with the marker of late endosomes/lysosomes Rab7 (Fig. 3, *A* and *B*) and almost no co-localization with Rab11, a marker of the long loop recycling pathway. Parallel experiments with the β_2-adrenergic receptor showed in agreement with previous findings a different postendocytic sorting pattern for this protein characterized by high co-localization with Rab11 and little co-localization with Rab7 (Fig. 3, *C* and *D*). This would also be expected for a protein well known to efficiently recycle via the long loop recycling pathway

(30). Importantly, our observations were based on the use of the same antibody epitope (FLAG) and antibody (M1), supporting that the differences found between TacSERT and β2-AR are indeed reflecting different properties between the two analyzed proteins. Sorting of constitutively internalized SERT to late endosomes and lysosomes was further supported by a profound co-localization between TacSERT or HA-SERT and the lysosomal marker LysoTracker but little co-localization between TacSERT or HA-SERT and transferrin. Others have likewise shown limited overlap between the transferrin receptor and SERT immunoreactivity in cells (43). Moreover, sorting of internalized SERT primarily to late endosomes was supported by labeling of hSERT with JHC1-64, showing that the internalized hSERT·JHC1-64 complex almost exclusively co-localized with Rab7-positive vesicles. Similarly, inhibitors of lysosomal degradation increased the amount of intracellular biotinylated SERT in our reversible biotinylation assay, consistent with targeting of a significant fraction of internalized transporter to degradation during the incubation period. The application of a pulse-chase biotinylation experiment using a nonreducible biotinylation experiment also supported that a significant fraction of SERT upon internalization was targeted to lysosomal degradation (Fig. 10*B*).

Internalized membrane proteins are initially targeted to early endosomes where cargo for lysosomal degradation is separated from the cargo used for recycling. It was therefore not surprising to see that both TacSERT and β_2-AR displayed some co-localization with Rab4. Interestingly, Rab4 mediates transfer from the early endosomes to a fast recycling pathway (short loop recycling pathway) distinct from the slow Rab11-sensitive recycling pathway. It has previously been suggested that constitutively internalized DAT to some extent take advantage of this fast pathway of recycling (17). Furthermore, in a recent study on the dopamine D2 receptor, it was shown that constitutive recycling of dopamine D2 receptor, and hence steady state surface levels, is sensitive to Rab4, whereas agonist-dependent recycling is sensitive to Rab11 (44). Because the transit time in rapid recycling of Rab4-positive endosomes was estimated to occur with a $t_{1/2}$ of 1–2 min (45), a decrease in TacSERT surface expression would be expected upon treatment with the recycling blocker monensin if the steady state level of surface SERT was dependent on rapid recycling. We observed, however, no significant decrease in TacSERT surface expression over 1 h of monensin treatment, arguing against significant recycling of SERT at least in the cellular system studied. Our reversible biotinylation assay also provided data arguing against significant recycling because incubation with monensin did not increase the amount of intracellular biotinylated protein during the incubation period as compared with leupeptin alone. Nonetheless, it is important to note that none of our experimental approaches exclude that a fraction of SERT undergoes recycling; our data only suggest that in the cell systems studied SERT appears to sort primarily to a degradative pathway.

In a previous study performed in our laboratory, constitutive internalization of DAT was visualized in primary cultures of dopaminergic neurons. By use of the fluorescent cocaine analog JHC1-64 to label surface-resident DAT, labeled DAT was shown to accumulate in intracellular compartments in the soma over time (10). Lentiviral transduction was used to express the EGFP-Rabs, and confocal images showed that constitutively internalized endogenous DAT was primarily sorted to the late endosomal/lysosomal pathway. This was in accordance with the sorting pattern observed for DAT transiently expressed in neuronal cell lines (17). We likewise tried to study SERT in its native environment. Accordingly, we established primary cultures of rat serotonergic raphe neurons. However, staining with an anti-SERT antibody revealed a distribution that favors the neurites with very low surface staining at the soma.[4] This is in accordance with an earlier electron microscopy study showing that plasma membrane SERT immunoreactivity preferentially localizes to the axonal membranes (46). However, because of the limited thickness of the axons and the relatively homogeneous distribution of SERT,[4] we were not capable of discriminating between plasma membrane-localized and intracellularly localized SERT in the axons with the limitations in resolution given by confocal microscopy. Lentiviral transduction was applied to express TacSERT or HA-Tac and study SERT trafficking in neurons by antibody feeding experiments. Although efficient expression was observed in a fraction of the neurons in culture, no overlap was observed with the marker of serotonergic neurons, tryptophan hydroxylase. Similarly, we attempted to express the EGFP-Rabs by lentiviral transduction without success. Thus, we were not capable of confirming the data obtained in the neuronal cell line CAD in the primary serotonergic cultures. As described above, studies performed on DAT indicate that the sorting pattern observed in neuronal cell lines is representative of the sorting pattern of endogenous DAT in dopaminergic cultures. Nevertheless, we should note that a study by Sorkin and co-workers (47) revealed that DAT might be sorted differentially in axonal or somatodendritic parts of the dopaminergic neurons, thus emphasizing the importance of future studies of SERT trafficking in neuronal cultures.

In conclusion, we show that SERT is subject to marked constitutive internalization. In addition, we show that upon internalization, SERT is sorted primarily to late endosomes and lysosomal compartments indicating that internalized SERT is destined for degradation rather than stored in recycling endosomes. It remains to be determined how postendocytic sorting affects SERT distribution and plasma membrane availability in neurons and, ultimately, how it affects serotonergic neurotransmission.

Acknowledgments—The fluorescent cocaine analog JHCl-64 was kindly provided by Professor Amy Hauck Newman at the National Institute on Drug Abuse, Baltimore, MD. We thank Anette Dencker Kaas for excellent technical assistance.

REFERENCES

1. Bröer, S., and Gether, U. (2012) The solute carrier 6 family of transporters. *Br. J. Pharmacol.* **167,** 256–278
2. Chen, N. H., Reith, M. E., and Quick, M. W. (2004) Synaptic uptake and beyond: the sodium- and chloride-dependent neurotransmitter transporter family SLC6. *Pflugers Arch.* **447,** 519–531

[4] T. N. Jørgensen and U. Gether, unpublished observations.

3. Kristensen, A. S., Andersen, J., Jørgensen, T. N., Sørensen, L., Eriksen, J., Loland, C. J., Strømgaard, K., and Gether, U. (2011) SLC6 neurotransmitter transporters: structure, function, and regulation. *Pharmacol. Rev.* **63,** 585–640
4. Yamashita, A., Singh, S. K., Kawate, T., Jin, Y., and Gouaux, E. (2005) Crystal structure of a bacterial homologue of Na^+/Cl^--dependent neurotransmitter transporters. *Nature* **437,** 215–223
5. Penmatsa, A., Wang, K. H., and Gouaux, E. (2013) X-ray structure of dopamine transporter elucidates antidepressant mechanism. *Nature* **503,** 85–90
6. Qian, Y., Galli, A., Ramamoorthy, S., Risso, S., DeFelice, L. J., and Blakely, R. D. (1997) Protein kinase C activation regulates human serotonin transporters in HEK-293 cells via altered cell surface expression. *J. Neurosci.* **17,** 45–57
7. Ramamoorthy, S., Giovanetti, E., Qian, Y., and Blakely, R. D. (1998) Phosphorylation and regulation of antidepressant-sensitive serotonin transporters. *J. Biol. Chem.* **273,** 2458–2466
8. Ramamoorthy, S., Shippenberg, T. S., and Jayanthi, L. D. (2011) Regulation of monoamine transporters: role of transporter phosphorylation. *Pharmacol. Ther.* **129,** 220–238
9. Sager, J. J., and Torres, G. E. (2011) Proteins interacting with monoamine transporters: current state and future challenges. *Biochemistry* **50,** 7295–7310
10. Eriksen, J., Rasmussen, S. G., Rasmussen, T. N., Vaegter, C. B., Cha, J. H., Zou, M. F., Newman, A. H., and Gether, U. (2009) Visualization of dopamine transporter trafficking in live neurons by use of fluorescent cocaine analogs. *J. Neurosci.* **29,** 6794–6808
11. Fornés, A., Núñez, E., Alonso-Torres, P., Aragón, C., and López-Corcuera, B. (2008) Trafficking properties and activity regulation of the neuronal glycine transporter GLYT2 by protein kinase C. *Biochem. J.* **412,** 495–506
12. Loder, M. K., and Melikian, H. E. (2003) The dopamine transporter constitutively internalizes and recycles in a protein kinase C-regulated manner in stably transfected PC12 cell lines. *J. Biol. Chem.* **278,** 22168–22174
13. Dautry-Varsat, A., Ciechanover, A., and Lodish, H. F. (1983) pH and the recycling of transferrin during receptor-mediated endocytosis. *Proc. Natl. Acad. Sci. U.S.A.* **80,** 2258–2262
14. Tsao, P. I., and von Zastrow, M. (2000) Type-specific sorting of G protein-coupled receptors after endocytosis. *J. Biol. Chem.* **275,** 11130–11140
15. Beguinot, L., Lyall, R. M., Willingham, M. C., and Pastan, I. (1984) Down-regulation of the epidermal growth factor receptor in KB cells is due to receptor internalization and subsequent degradation in lysosomes. *Proc. Natl. Acad. Sci. U.S.A.* **81,** 2384–2388
16. Sorkina, T., Hoover, B. R., Zahniser, N. R., and Sorkin, A. (2005) Constitutive and protein kinase C-induced internalization of the dopamine transporter is mediated by a clathrin-dependent mechanism. *Traffic* **6,** 157–170
17. Eriksen, J., Bjørn-Yoshimoto, W. E., Jørgensen, T. N., Newman, A. H., and Gether, U. (2010) Postendocytic sorting of constitutively internalized dopamine transporter in cell lines and dopaminergic neurons. *J. Biol. Chem.* **285,** 27289–27301
18. Cha, J. H., Zou, M. F., Adkins, E. M., Rasmussen, S. G., Loland, C. J., Schoenenberger, B., Gether, U., and Newman, A. H. (2005) Rhodamine-labeled 2β-carbomethoxy-3β-(3,4-dichlorophenyl)tropane analogues as high affinity fluorescent probes for the dopamine transporter. *J. Med. Chem.* **48,** 7513–7516
19. Sucic, S., Dallinger, S., Zdrazil, B., Weissensteiner, R., Jørgensen, T. N., Holy, M., Kudlacek, O., Seidel, S., Cha, J. H., Gether, U., Newman, A. H., Ecker, G. F., Freissmuth, M., and Sitte, H. H. (2010) The N terminus of monoamine transporters is a lever required for the action of amphetamines. *J. Biol. Chem.* **285,** 10924–10938
20. Tate, C. G., and Blakely, R. D. (1994) The effect of *N*-linked glycosylation on activity of the Na^+- and Cl^--dependent serotonin transporter expressed using recombinant baculovirus in insect cells. *J. Biol. Chem.* **269,** 26303–26310
21. Lavezzari, G., McCallum, J., Dewey, C. M., and Roche, K. W. (2004) Subunit-specific regulation of NMDA receptor endocytosis. *J. Neurosci.* **24,** 6383–6391
22. Brown, T. C., Correia, S. S., Petrok, C. N., and Esteban, J. A. (2007) Functional compartmentalization of endosomal trafficking for the synaptic delivery of AMPA receptors during long-term potentiation. *J. Neurosci.* **27,** 13311–13315
23. Qi, Y., Wang, J. K., McMillian, M., and Chikaraishi, D. M. (1997) Characterization of a CNS cell line, CAD, in which morphological differentiation is initiated by serum deprivation. *J. Neurosci.* **17,** 1217–1225
24. Madsen, K. L., Eriksen, J., Milan-Lobo, L., Han, D. S., Niv, M. Y., Ammendrup-Johnsen, I., Henriksen, U., Bhatia, V. K., Stamou, D., Sitte, H. H., McMahon, H. T., Weinstein, H., and Gether, U. (2008) Membrane localization is critical for activation of the PICK1 BAR domain. *Traffic* **9,** 1327–1343
25. Jayanthi, L. D., Samuvel, D. J., Blakely, R. D., and Ramamoorthy, S. (2005) Evidence for biphasic effects of protein kinase C on serotonin transporter function, endocytosis, and phosphorylation. *Mol. Pharmacol.* **67,** 2077–2087
26. Samuvel, D. J., Jayanthi, L. D., Bhat, N. R., and Ramamoorthy, S. (2005) A role for p38 mitogen-activated protein kinase in the regulation of the serotonin transporter: evidence for distinct cellular mechanisms involved in transporter surface expression. *J. Neurosci.* **25,** 29–41
27. van der Bliek, A. M., Redelmeier, T. E., Damke, H., Tisdale, E. J., Meyerowitz, E. M., and Schmid, S. L. (1993) Mutations in human dynamin block an intermediate stage in coated vesicle formation. *J. Cell Biol.* **122,** 553–563
28. Stenmark, H. (2009) Rab GTPases as coordinators of vesicle traffic. *Nat. Rev. Mol. Cell Biol.* **10,** 513–525
29. Jovic, M., Sharma, M., Rahajeng, J., and Caplan, S. (2010) The early endosome: a busy sorting station for proteins at the crossroads. *Histol. Histopathol.* **25,** 99–112
30. Moore, R. H., Millman, E. E., Alpizar-Foster, E., Dai, W., and Knoll, B. J. (2004) Rab11 regulates the recycling and lysosome targeting of β2-adrenergic receptors. *J. Cell Sci.* **117,** 3107–3117
31. Yudowski, G. A., Puthenveedu, M. A., Henry, A. G., and von Zastrow, M. (2009) Cargo-mediated regulation of a rapid Rab4-dependent recycling pathway. *Mol. Biol. Cell* **20,** 2774–2784
32. Mollenhauer, H. H., Morré, D. J., and Rowe, L. D. (1990) Alteration of intracellular traffic by monensin; mechanism, specificity and relationship to toxicity. *Biochim. Biophys Acta* **1031,** 225–246
33. Sorkina, T., Miranda, M., Dionne, K. R., Hoover, B. R., Zahniser, N. R., and Sorkin, A. (2006) RNA interference screen reveals an essential role of Nedd4-2 in dopamine transporter ubiquitination and endocytosis. *J. Neurosci.* **26,** 8195–8205
34. Anderluh, A., Klotzsch, E., Reismann, A. W., Brameshuber, M., Kudlacek, O., Newman, A. H., Sitte, H. H., and Schütz, G. J. (2014) Single molecule analysis reveals coexistence of stable serotonin transporter monomers and oligomers in the live cell plasma membrane. *J. Biol. Chem.* **289,** 4387–4394
35. Adachi, K., Ichinose, T., Takizawa, N., Watanabe, K., Kitazato, K., and Kobayashi, N. (2007) Inhibition of betanodavirus infection by inhibitors of endosomal acidification. *Arch. Virol.* **152,** 2217–2224
36. Holton, K. L., Loder, M. K., and Melikian, H. E. (2005) Nonclassical, distinct endocytic signals dictate constitutive and PKC-regulated neurotransmitter transporter internalization. *Nat. Neurosci.* **8,** 881–888
37. Roche, K. W., Standley, S., McCallum, J., Dune Ly, C., Ehlers, M. D., and Wenthold, R. J. (2001) Molecular determinants of NMDA receptor internalization. *Nat. Neurosci.* **4,** 794–802
38. Rasmussen, T. N., Plenge, P., Bay, T., Egebjerg, J., and Gether, U. (2009) A single nucleotide polymorphism in the human serotonin transporter introduces a new site for *N*-linked glycosylation. *Neuropharmacology* **57,** 287–294
39. Ramamoorthy, S., and Blakely, R. D. (1999) Phosphorylation and sequestration of serotonin transporters differentially modulated by psychostimulants. *Science* **285,** 763–766
40. Ramamoorthy, J. D., Ramamoorthy, S., Papapetropoulos, A., Catravas, J. D., Leibach, F. H., and Ganapathy, V. (1995) Cyclic AMP-independent up-regulation of the human serotonin transporter by staurosporine in choriocarcinoma cells. *J. Biol. Chem.* **270,** 17189–17195
41. Austin, C. D., Wen, X., Gazzard, L., Nelson, C., Scheller, R. H., and Scales,

S. J. (2005) Oxidizing potential of endosomes and lysosomes limits intracellular cleavage of disulfide-based antibody-drug conjugates. *Proc. Natl. Acad. Sci. U.S.A.* **102,** 17987–17992
42. Matthies, H. J., Moore, J. L., Saunders, C., Matthies, D. S., Lapierre, L. A., Goldenring, J. R., Blakely, R. D., and Galli, A. (2010) Rab11 supports amphetamine-stimulated norepinephrine transporter trafficking. *J. Neurosci.* **30,** 7863–7877
43. Müller, H. K., Wiborg, O., and Haase, J. (2006) Subcellular redistribution of the serotonin transporter by secretory carrier membrane protein 2. *J. Biol. Chem.* **281,** 28901–28909
44. Li, Y., Roy, B. D., Wang, W., Zhang, L., Zhang, L., Sampson, S. B., Yang, Y., and Lin, D. T. (2012) Identification of two functionally distinct endosomal recycling pathways for dopamine D(2) receptor. *J. Neurosci.* **32,** 7178–7190
45. Hao, M., and Maxfield, F. R. (2000) Characterization of rapid membrane internalization and recycling. *J. Biol. Chem.* **275,** 15279–15286
46. Tao-Cheng, J. H., and Zhou, F. C. (1999) Differential polarization of serotonin transporters in axons versus soma-dendrites: an immunogold electron microscopy study. *Neuroscience* **94,** 821–830
47. Rao, A., Simmons, D., and Sorkin, A. (2011) Differential subcellular distribution of endosomal compartments and the dopamine transporter in dopaminergic neurons. *Mol. Cell Neurosci.* **46,** 148–158